The Buoyancy and Wind-Driven Ventilated Thermocline*

JOSEPH PEDLOSKY

Woods Hole Oceanographic Institution, Woods Hole, MA 02543

(Manuscript received 1 November 1985, in final form 27 December 1985)

ABSTRACT

An analytical study of the combined wind-driven and buoyancy-driven thermocline problem is presented. The analysis is an extension of the ventilated thermocline model of Luyten et al.

An exact solution for the ventilated region of the subtropical gyre is found under the condition that the *ratio* of the buoyancy flux to Ekman pumping is a function of latitude alone. It demonstrates the general westward shift of streamlines when the subtropical gyre is heated and the enlargement of the eastern shadow zone.

The flow in the shadow zone is described, in most instances, for the case of relatively small buoyancy flux. It is shown that the shadow zone, now in motion due to buoyancy forcing, splits into two zones. There is a broad eastward zone in which the deep flow is northeastward and a narrow zone between this branch and the ventilated fluid in which the shadow zone flow is returned in a relatively swift current nearly preserving potential vorticity. For buoyancy/Ekman flux ratios which are nearly independent of position, the eastern branch of the shadow zone circulation lacks a beta spiral and the meridional transport can be simply calculated as a direct response to the heating.

For sufficiently large heating, the model predicts pinch-off of the cold water layer along a latitude circle in the ventilated zone, south of which the solution loses validity.

1. Introduction

The theory of the Ventilated Thermocline (Luyten et al., 1983, hereafter LPS) describes a model of the oceanic thermocline in which the driving mechanism for the subsurface, geostrophic circulation is the fluid pumped out of the upper mixed layer, i.e., the Ekman velocity w_E. The Ekman velocity is directly related to the wind stress curl and thus the LPS theory describes an oceanic thermocline whose flow is determined by the supposedly known distribution of wind stress. The density field enters the dynamics by the specification of the surface density field, i.e., the lines on which the interfaces between layers of constant density outcrop. Although the density field is dynamically active, e.g., by providing buoyancy forces and producing thermal wind currents, it is considered thermodynamically passive in the model of LPS. That is, density is considered a conserved quantity. In the context of the layered model of LPS, this is equivalent to the constraint that fluid not cross interfaces between layers of constant density in the region beneath the mixed layer. Such a transfer requires a change of density for each parcel being so transferred and consequently requires heat added or subtracted from the parcel to effect the change in density. Thus in LPS, the requirement of density conservation is equivalent to the absence of any heating (or buoyancy change) penetrating below the mixed layer. The exchange of heat within the mixed layer can be modeled within the confines of the adiabatic model as shown by Pedlosky et al., 1984.

Recently, there has been a revival of interest in the role of deep buoyancy fluxes in the dynamics of the thermocline. Luyten and Stommel (1986a,b) have studied the dynamics of a two-moving-layer model in which the buoyancy flux, i.e., the internal heating, is represented by a specified mass flux between the lower and upper moving layers. This mass flux is prescribed in the same manner as the Ekman pumping, i.e., as a supposedly known function of geographical position although admittedly, the actual relation between this buoyancy forcing and any external observable, e.g., surface heat flux is far less well understood than the relation between w_E and the wind stress.

Luyten and Stommel (1986a) used an ingenious reformulation of the geostrophic equations in the two-layer model to derive a single quasi-linear partial differential equation for the thermocline depth. In their formulation, the characteristics of the resulting hyperbolic equation depend only on the total Sverdrup transport, known a priori, and the layer thicknesses. The fact that the characteristics do not depend on *derivatives* of layer depth in their formulation renders numerical integration of the resulting equations extremely easy and economical. (It is interesting to note that the device used by Luyten and Stommel is the generalization of the technique used by Rhines and Young, 1981, in which isopleths of quasi-geostrophic

* Woods Hole Oceanographic Institution Contribution No. 6070.

potential vorticity are rewritten in terms of the barotropic streamfunction and then, as a known quantity, used to define domains of potential vorticity homogenization.)

Although the Luyten and Stommel approach is intrinsically limited to a two-layer model, the results of their numerical calculations are of great interest and raise many issues about the relation between the wind-driven and buoyancy-driven circulations. The purpose of the present paper is to present analytical solutions to the combined buoyancy and wind-driven circulation problem. The analysis is limited entirely to the subtropical gyre. The subpolar gyre problem presents a conceptual difficulty due to its sensitivity to data required on the western boundary of the mid-ocean flow, data which is hard to prescribe uniquely.

In section 2, the equations for the n-layer model are presented. An exact solution for the two- and three-moving-layer problem is then presented. The solution applies *only* to the ventilated portion of the subtropical gyre but is valid for arbitrarily large values of the interfacial mass flux relative to the Ekman flux. Regardless of the sign of the buoyancy flux, the meridional velocity is determined only by the sense of the Sverdrup transport, e.g., it is equatorward. The buoyancy flux plays an important role, however, in determining the eastern boundary of the ventilated zone, i.e., the western edge of the shadow zone described in LPS. It is shown that buoyancy fluxes associated with heating of the subtropical gyre shift ventilated streamlines westward and so expand the extent of the shadow zone.

Heating or cooling of the gyre tends to produce "pinch-off" of an internal density layer and for the cases described herein, this occurs on latitude circles in the ventilated zone as long as the *ratio* of the buoyancy flux to the Ekman flux depends only on latitude.

Section 3 describes the circulation driven by buoyancy fluxes within the shadow zone. For relatively small buoyancy flux, it is shown that the circulation in the shadow zone due to heating consists of a broad northeastward branch (a direct cell in the terminology of Luyten and Stommel, 1986b) whose southwestward return flow is limited to a narrow zone on the eastern edge of the ventilated flow. In the northeastward branch, the twisting terms in the potential vorticity equation vanish when the ratio of the buoyancy flux to Ekman flux is essentially independent of position in the shadow zone. This allows a most simple relation between the buoyancy flux and the transport in this branch of the buoyancy-driven current to be derived. It is further shown in section 3 that the vanishing of the twisting terms in the northeastward branch also occurs for large values of the buoyancy flux.

In many ways, the analytical approach followed in this paper is less flexible than the numerical approach pioneered by Luyten and Stommel. Nevertheless, having in hand explicitly analytical representation of major features of the circulation is of obvious value.

2. The model

The physical model is shown in Fig. 1. The model ocean consists of N layers with thicknesses $h_1, h_2, \ldots h_N$, the interfaces of which intersect the sea surface of latitudes y_n where the Coriolis parameter is f_n. The density of each layer is a constant ρ_n. Frictional coupling between the layers is ignored but mass can pass through the interfaces at a rate U_n where

$$U_n = w_n + \mathbf{u}_{nH} \cdot \nabla Z_n \tag{2.1}$$

where w_n is the Eulerian vertical velocity, $\mathbf{u}_{nH}$ is the horizontal velocity and Z_n is the depth of the nth interface; U_n is an entrainment velocity and represents the rate at which fluid with density ρ_{n+1} is converted to fluid of density ρ_n. This, of course, requires nonadiabatic processes to be at work at the interface and is the model used for the manifestation of internal heating. In (2.1) U_n is evaluated at $z = -Z_n$. Since U_n must be continuous across the interface, it follows that (2.1) is equivalent to

$$U_n = w_{n+1} + \mathbf{u}_{n+1H} \cdot \nabla Z_n \quad \text{at} \quad z = -Z_n \tag{2.2}$$

from which it follows, with the aid of the geostrophic relations introduced below that $w_n = w_{n+1}$ at each interface.

The integral of the equation of mass conservation over each layer yields, for steady flows,

$$\nabla_H \cdot (\mathbf{u}_n h_n) = U_n - U_{n-1} \tag{2.3}$$

where the $\mathbf{u}_n$ are independent of z as required by geostrophy and the hydrostatic approximation. Where the upper surface of a layer is exposed to the sea surface, the mass flux U_{surface} becomes equal to the Ekman pumping w_E.

Within each layer the motion is geostrophic and hydrostatic, i.e., with standard notation

$$\rho_n f u_n = -\frac{\partial p_n}{\partial y}$$

$$\rho_n f v_n = \frac{\partial p_n}{\partial x}$$

$$\rho_n g = -\frac{\partial p_n}{\partial z}. \tag{2.4a,b,c}$$

The Sverdrup vorticity equation follows directly as

$$\beta v_n = f \frac{\partial w_n}{\partial z} \tag{2.5}$$

whose sum over all the moving layers yields

$$\beta \sum_n h_n v_n = f w_E(x, y) \tag{2.6}$$

where it has been assumed that the velocity field does not interact with the ocean bottom. Note that the Sverdrup relation (2.6) is independent of the inter-layer mass fluxes.

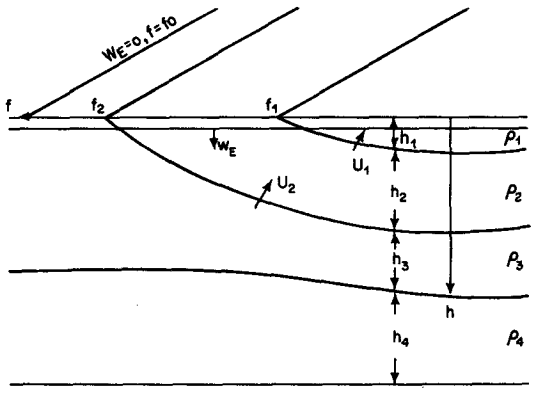

FIG. 1. The physical model in schematic cross section. The latitudes of density outcrop are (in terms of Coriolis parameter) f_2 and f_1. The Ekman pumping is negative and vanishes at $f = f_0$. The cross-interface mass fluxes are U_1 and U_2.

When (2.5) is integrated over a single layer, we obtain the potential vorticity equation for the nth layer in the form

$$u_n \frac{\partial}{\partial x}\frac{f}{h_n} + v_n \frac{\partial}{\partial y}\frac{f}{h_n} = -\frac{f}{h_n^2}(U_n - U_{n-1}) \quad (2.7)$$

where $f = 2\Omega \sin\theta$.

Should the mass fluxes U_n and U_{n-1} vanish, then $q_n = f/h_n$, the potential vorticity of the nth layer, would be conserved. The presence of a net flux across the layer boundaries, i.e., of a "divergence," $(U_n - U_{n-1})/h_n$ of the cross-interface mass flux will lead to a decrease of potential vorticity at a rate equal to the product of this divergence with the potential vorticity.

In the cases to be described below, no more than three moving layers will be considered. Hence, layer 4 will always be at rest. The outcrop lines will be taken as latitude circles. The Ekman flux vanishes on $f = f_0$ and is negative for $f < f_0$. In the region $f_2 \leqslant f \leqslant f_0$, there is one moving layer, layer 3, driven only by Ekman pumping. The depth of the base of layer 3 is called h and in the zone $f_2 \leqslant f \leqslant f_0$,

$$v_3 = \frac{\gamma_3}{f}\frac{\partial h_3}{\partial x} \quad (2.8a)$$

$$u_3 = -\frac{\gamma_3}{f}\frac{\partial h_3}{\partial y} \quad (2.8b)$$

where $\gamma_n = g(\rho_{n+1} - \rho_n)/\rho_0$ where ρ_0 is the average density in the model and where $\rho_{n+1} - \rho_n \ll \rho_0$ for all n. As shown in LPS, the Sverdrup relation (2.6) is sufficient in this region to find h, i.e., in $f_2 \leqslant f \leqslant f_0$

$$h_3 = h = [D_0^2(x, y) + H_3^2]^{1/2} \quad (2.9a)$$

where

$$D_0^2 \equiv -\frac{2f^2}{\gamma_3 \beta}\int_x^{X_E} w_E(x', y)dx'. \quad (2.9b)$$

In (2.9a, b), H_3 is the constant thickness of layer 3 on the eastern wall at $x = X_E$ where we assume the geostrophic zonal velocity must vanish.

Consider now the flow in the region $f_1 \leqslant f \leqslant f_2$. If $w_E < 0$, all the fluid in the region $f_2 \leqslant f \leqslant f_0$ will be forced southward by the Ekman pumping and at $f = f_2$, the fluid in layer 3 will be covered by layer 2 after it subducts. From that point on, the fluid is subjected to a buoyancy forcing represented by the mass flux U_2 which causes fluid to leave layer 3 and be entrained in layer 2, suffering in the process a decrease of density $\rho_3 - \rho_2$. In this case (2.7) becomes

$$u_3 \frac{\partial}{\partial x}\frac{f}{h_3} + v_3 \frac{\partial}{\partial y}\frac{f}{h_3} = \frac{f}{h_3^2}U_2 \quad (2.10)$$

where

$$\begin{Bmatrix} U_3 \\ V_3 \end{Bmatrix} = \frac{\gamma_3}{f}\begin{Bmatrix} -\partial/\partial y \\ \partial/\partial x \end{Bmatrix} h$$

where $h = h_2 + h_3$. Thus (2.10) may be written

$$\frac{\partial h}{\partial x}\frac{\partial}{\partial y}\frac{f}{h_3} - \frac{\partial h}{\partial y}\frac{\partial}{\partial x}\frac{f}{h_3} = \frac{f^2}{h_3^2}\frac{U_2}{\gamma_3}. \quad (2.11)$$

The Sverdrup relation (2.6) in this region may be written (LPS) as

$$h^2 + \Gamma_2 h_2^2 = D_0^2 + H_3^2 \quad (2.12)$$

where $\Gamma_n \equiv \gamma_n/\gamma_3$. Note that (2.12) assumes that the depth of layer 2 must vanish on $x = X_E$ to avoid geostrophic flow through the eastern boundary.

In LPS, U_2 was zero and (2.11) required that potential vorticity be constant along streamlines in layer 3. That is, if U_2 were zero, (2.11) requires that f/h_3 be a function only of h. LPS relied heavily on this adiabatic feature to find a solution to (2.11) and (2.12). In that case, it was shown that in $f_1 \leqslant f \leqslant f_2$ the relations

$$\boxed{\begin{aligned} h_2 &= \theta(f)h \\ h_3 &= (1 - \theta)h \end{aligned}} \quad (2.13a, b)$$

held where $\theta = (1 - f/f_2)$, from which it followed from (2.12) that in this zone

$$\boxed{h = (D_0^2 + H_3^2)^{1/2}/(1 + \Gamma_2\theta^2)^{1/2}}. \quad (2.14)$$

Clearly, when U_2 differs from zero, potential vorticity is no longer conserved and the particular method of analysis used in LPS must be abandoned. Remarkably, however, under the condition that U_2/w_E be a function of latitude alone, the solution (2.13a, b) and (2.14) will still be valid except that now θ is a more complicated function of latitude to be described below. Thus if

$$b_2 \equiv U_2/w_e \quad (2.15)$$

is a function only of latitude (or f) then (2.13a, b) and (2.14) will satisfy (2.11) and (2.12) if $\theta(f)$ is a solution

of the relatively simple first-order ordinary differential equation,

$$f\frac{d\theta}{df} + (1-\theta) - b_2(f)(1+\Gamma_2\theta^2) = 0 \qquad (2.16)$$

as may be verified by substituting (2.13a, b) and (2.14) into (2.11) and (2.12).

The condition that b_2 be a function of latitude alone is not particularly an irksome one since in most calculations done to date w_E and U_2 are themselves functions of latitude alone (e.g., Luyten and Stommel, 1986b). Here they may be individually dependent on longitude as long as their ratio is not.

The initial condition for (2.16) is that on $f = f_2$, h_2 vanish so that

$$\theta(f_2) = 0. \qquad (2.17)$$

Note that if b_2 is identically zero, the solution of (2.16) subject to (2.17) is simply

$$\theta = 1 - \frac{f}{f_2}$$

which recovers the result of LPS.

For general $b_2(f)$, (2.16) requires a numerical solution, yet the numerical integration required is so trivial that it seems justified to call (2.13a, b) and (2.14) an exact solution. More significantly, the structure of the analytical solution is extremely revealing. It follows from (2.14) that

$$v_3 = \frac{\gamma_3}{f}\frac{\partial h}{\partial x} = \gamma_3 \frac{h}{2f(D_0^2 + H_3^2)}\frac{\partial D_0^2}{\partial x} \qquad (2.18)$$

and so the meridional velocity is *always* equatorward in the ventilated zone regardless of the size or *sign* of the buoyancy flux. Thus, although the fluid in layer 3 may be heated in the ventilated zone, the flow in that layer must be equatorward or indirect in the terminology of Luyten and Stommel (1986b).

If $b_2 < 0$, (2.16) shows that θ must increase as f decreases at a rate greater than that which occurs in the adiabatic case treated by LPS. When θ reaches unity, (2.13) shows that the thickness of layer 3 goes to zero. When $b_2 = 0$, this occurs at the equator, i.e., at the limit of the domain of the problem. For $b_2 < 0$, this can occur for $f > 0$. Figure 2 shows the solution for θ in the case

$$b_2 = B_{20}\frac{f}{f_2}\left(1 - \frac{f}{f_2}\right)$$

$$B_{20} = -1/2, \qquad (2.19)$$

i.e., for a buoyancy flux which starts at zero at the outcrop latitude and vanishes also at the equator. In this case, I have chosen $f_1 = 0$, reducing the model to a two-moving-layer model. Note that θ everywhere exceeds the LPS value and reaches unity at $f/f_2 \approx 0.14$. The solution fails south of this point but the solution

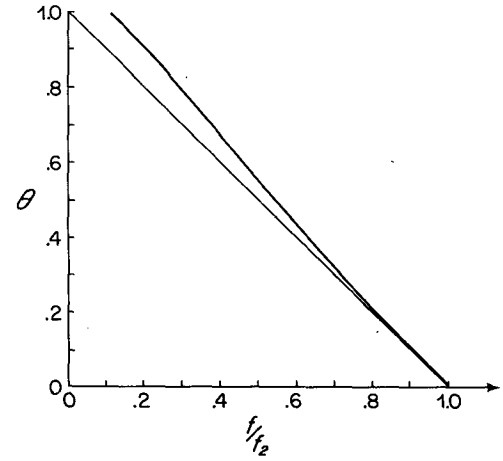

FIG. 2. The solution for $\theta(f)$ when there are only two moving layers (i.e., when $f_1 \to 0$) for $b_2 = 0.5f/f_2(1 - f/f_2)$.

predicts that pinch-off will occur and must always occur on a latitude circle. To investigate the position of pinch-off as a function of the buoyancy flux, it is useful to consider the somewhat contrived case where

$$b_2 = U_2/w_E = b_0$$

i.e., where b_0 *is a constant*. In that case, (2.16) can be integrated directly.

Define

$$R^2 = b_0(b_0 - 1)\Gamma_2 - 1/4.$$

If $R^2 > 0$, the solution to (2.16) is given by

$$\theta b_0\Gamma_2 = -\frac{1}{2} + R\tan\left[R\ln\frac{f}{f_2} + \tan^{-1}\left(\frac{1}{2R}\right)\right]$$

while if $R^2 < 0$

$$\theta = \frac{2(1-b_0)[1-(f/f_2)^s]}{(1+s)+(f/f_2)^s(s-1)}$$

where $s^2 = -4R^2$. The condition for pinch-off is simply $\theta = 1$. Fig. 3 shows how the latitude of pinch-off depends on the magnitude of the buoyancy flux. The larger the buoyancy flux, the closer pinch-off occurs to the outcrop line. Note that within the ventilated zone the latitude of pinch-off is *independent* of H_3, the depth of the lower layer at $f = f_0$.

However, the existence of the shadow zone, described in section 3, and whose extent does depend on H_3, will determine to what extent the pinch-off will actually occur in the physical domain of the problem, i.e., for $X_w \leq x \leq X_E$ where X_w is the coordinate of the oceanic western boundary.

It is important to bear in mind that a large part of the solution structure is contained in the factor $(D_0^2 + H_3^2)$ in (2.14). This means that much of the overall flow structure is not qualitatively altered by the buoyancy flux *in the ventilated zone*, e.g., the formula (2.18) for v_3.

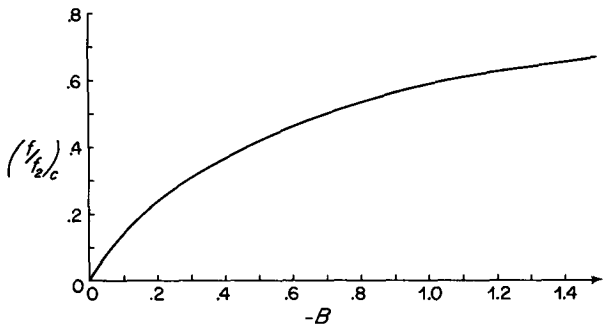

FIG. 3. The latitude of pinch-off in the two-layer model as a function of b_2 for the case where $U_2/W_e < 0$ and independent of latitude.

The zonal velocity is more sensitive to the buoyancy flux. It follows from geostrophy and (2.16) that in the ventilated zone

$$u_3 = -\frac{\gamma_3}{f}\frac{\partial h}{\partial y} = -\frac{\gamma_3}{f}\left\{\frac{h}{2}\frac{\partial D_0^2}{\partial y}\frac{1}{(D_0^2 + H_3^2)} - \frac{\beta\Gamma_2 h_2}{f}\left[b_2 - \frac{hh_3}{(D_0^2 + H_3^2)}\right]\right\}.$$

When the subtropical gyre is heated, $b_2 < 0$, and the buoyancy forcing contributes a *westward* addition to the fluid motion. In general, heating will shift the streamlines of the ventilated flow *westward* with respect to the purely wind-driven case. The trajectory of a fluid column in layer 3 which originates at the outcrop line, at $f = f_2$, and at the longitude $x = \xi$ will be given by the implicit relation $h(x,f) = h(\xi, f_2)$, which with (2.14) yields

$$D_0^2(x,f) = H_3^2\Gamma_2\theta^2 + D_0^2(\xi, f_2)(1 + \Gamma_2\theta^2). \quad (2.20)$$

Since (1) D_0^2 is an increasing function of $X_E - x$ (i.e., 2.9b) and (2) since θ increases with decreasing $b_2(f)$ it follows that each trajectory must be displaced westward by heating ($b_2 < 0$).

Before proceeding to the completion of the three-layer solution in the ventilated zone, i.e., in the region $0 \leq f \leq f_1$, it is interesting to consider the case where the subtropical gyre becomes *cooled*. Although a less natural choice of forcing, the result is quite interesting. Consider the case where $b_2(f)$ has the same form as (2.19) but where now, $B_{20} > 0$. Then fluid transits from layer 2 into layer 3 due to cooling. Figure 4a shows $\theta(f)$ while Fig. 4b shows the layer depths when scaled by the factor $(D_0^2 + H_3^2)^{1/2}$. In the case shown, $\Gamma_2 = 1$ and $B_{20} = 4.5$. Note that the peak of the cooling, or more exactly of the ratio U_2/w_e at $f/f_2 = \frac{1}{2}$ tends to produce a separation of the warm water region into two pools while the cold water region tends to remain relatively flat. Strong meridional gradients then arise near the equator where $b_2 \to 0$ and the conservation of q_3 demands that $h_3 \to 0$. For larger values of B_{20}, the warm pools would separate and the validity of the solution fails. It remains unclear to me, in both cases of strong heating and cooling, how to continue the analytical solution beyond the point of pinch-off.

Now consider the flow in the region $f \leq f_1$ where, in the ventilated zone, three layers are in motion. In this case the Sverdrup relation (2.6) becomes (LPS)

$$h^2 + \Gamma_2(h_1 + h_2)^2 + \Gamma_1 h_1^2 = D_0^2 + H_3^2. \quad (2.21)$$

The equation for layer 3 remains (2.11) while the equation for layer 2 is, from (2.7),

$$u_2\frac{\partial}{\partial x}\frac{f}{h_2} + v_2\frac{\partial}{\partial y}\frac{f}{h_2} = \frac{f}{h_2^2}(U_1 - U_2) \quad (2.22)$$

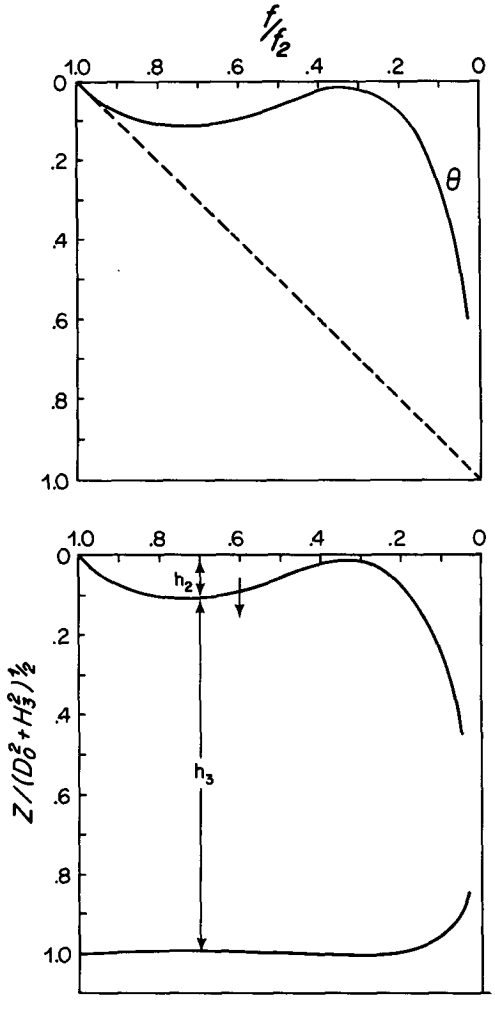

FIG. 4. (a) The function $\theta(f)$ for the case of *cooling*. $b_2(f) = 4.5f/f_2(1 - f/f_2)$ for the two-moving-layer model. $\Gamma_2 = 1$. The dotted line shows θ for the case $b_2 = 0$. (b) The layer depths for the cooling case. The depths are divided by the factor $(D_0^2 + H_3^2)^{1/2}$. Note the separation of the warm layer into two pools as a consequence of the cooling.

where (LPS)

$$\begin{Bmatrix} u_2 \\ v_2 \end{Bmatrix} = \frac{\gamma_3}{f} \begin{Bmatrix} -\partial/\partial y \\ \partial/\partial x \end{Bmatrix} [h + \Gamma_2(h_1 + h_2)] \quad (2.23)$$

where, of course, now, $h = h_1 + h_2 + h_3$.

Again guided by the *form* of the LPS solution and the condition imposed by the Sverdrup relation (2.21) a solution to the three-layer buoyancy, wind-driven problem can be found in the form

$$h_1 = \eta(f)h$$

$$h_2 = [\theta(f) - \eta(f)]h$$

$$h_3 = [1 - \theta(f)]h \quad (2.24a,b,c)$$

where

$$h = [(D_0^2 + H_3^2)/(1 + \Gamma_2\theta^2 + \Gamma_1\eta^2)]^{1/2} \quad (2.25)$$

as long as both $U_2/w_e \equiv b_2$ and $U_1/w_e \equiv b_1$ are functions only of latitude, i.e., of f. The forms (2.24) and (2.25) will satisfy (2.11), (2.21) and (2.22) if θ and η satisfy

$$f\frac{d\theta}{df} + (1 - \theta) - b_2(1 + \Gamma_2\theta^2 + \Gamma_1\eta^2) = 0 \quad (2.26)$$

$$\frac{d}{df}\left[\frac{\eta - \theta}{(1 + \Gamma_2\theta)f}\right] - \frac{(b_1 - b_2)}{f^2}\frac{(1 + \Gamma_2\theta^2 + \Gamma_1\eta^2)}{(1 + \Gamma_2\theta)^2} = 0, \quad (2.27a)$$

or equivalently

$$f(1 + \Gamma_2\theta)\frac{d\eta}{df} - \eta[2\Gamma_2\theta + (1 - \Gamma_2)] = -(1 + \Gamma_2\theta^2) + (1 + \Gamma_2\theta^2 + \Gamma_1\eta^2)(b_1 + b_2\Gamma_2\eta) \quad (2.27b)$$

where for (2.27), we use the condition $\eta = 0$ for $f \geq f_1$. If b_1 and b_2 vanish, then we can check that

$$\theta = 1 - \frac{f}{f_2}$$

$$\eta = \left(1 - \frac{f}{f_2}\right) - \left(1 - \frac{f_1}{f_2}\right)\frac{[1 + \Gamma_2(1 - f/f_2)]}{[1 + \Gamma_2(1 - f_1/f_2)]}\frac{f}{f_1}$$

reproducing the results of LPS.

It is quite easy to integrate (2.26) and (2.27) and Fig. 5 shows the result for the case where

$$b_2 = B_{20}\frac{f}{f_2}\left(1 - \frac{f}{f_2}\right)$$

$$b_1 = B_{10}\frac{f}{f_2}\left(1 - \frac{f}{f_1}\right).$$

Figure 5a shows the layer thicknesses scaled by $(D_0^2 + H_3^2)^{1/2}$, for the purely wind-driven case $b_1 = b_2 = 0$. Figure 5b shows the functions θ and η for the case where $B_{10} = -1$ and $B_{20} = -0.5$ for $\Gamma_1 = \Gamma_2 = 1$ while $f_1/f_2 = 0.5$. In this case the heating amplitude, or the buoyancy flux, decreases downward. In Fig. 5b, dotted lines show θ and η for the purely wind-driven case of LPS for comparison. Note that as in the two layer region the effect of heating is to increase θ and η and

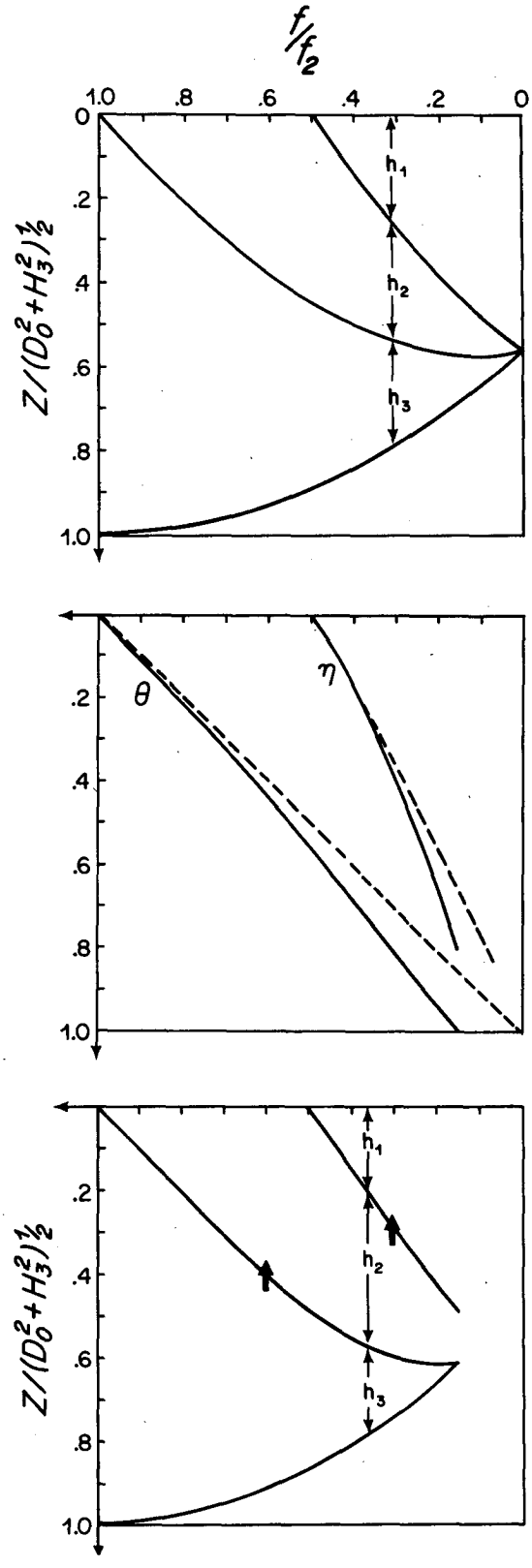

FIG. 5. (a) The scaled layer depths for the three-layer purely wind-driven case, $b_n = 0$. (b) The functions θ and η, for the case with heating $b_2 = -0.5f/f_2(1 - f/f_2)$, $b_1 = -f/f_2(1 - f/f_1)$. (c) The layer depths for the heated case of 5b.

since, again, θ reaches unity north of the equator, the model predicts pinch-off of the coldest moving layer, in this case for $f/f_2 = 0.15$. Figure 5c shows the scaled layer depths in this case. Again, the analytical solution cannot be continued south of the pinch-off latitude where fluid of density ρ_2 is now directly above fluid of density ρ_4. Obviously a buoyancy flux through the base of layer 2 would drive a weak circulation in layer 4 which should be put in motion south of the pinch-off latitude. This situation is reminiscent of the surfacing of isopycnals in the subpolar gyre found in LPS where deep layers become exposed to Ekman suction north of the outcrop line along which the superposed layer above is sucked to the surface.

It is useful at this point to consider in more detail the case when U_n/w_E is small. This will prove illuminating for several reasons. First, since the presence of the buoyancy term on the right-hand side of (2.7) is a *regular* perturbation of the problem, we can confidently expect that the small U_n solutions will capture the *qualitative* nature of the solution. Second, we can trade the restriction of small buoyancy flux for the condition that U_n/w_E be independent of longitude. This allows us to expand the qualitative character of the forcings considered. Finally, it will prove useful to have the small U_n solutions to check with the small b_n expansion of (2.16). This last point is useful since (2.13), (2.14) represents a proposed solution that seems to work and it is useful to check that it is the only solution which can be generated, at least for small U_n.

For simplicity, I will restrict attention to the case $f_1 \to 0$ so the model ocean contains only two moving layers, i.e., layers 2 and 3.

For small U_n, the solution may be generated as an asymptotic series in each variable, for example,

$$h = h^{(0)} + h^{(1)} \tag{2.28}$$

where superscripts refer to orders in the small buoyancy expansion and

$$h^{(1)}/h^{(0)} = \mathrm{O}(b) \ll 1. \tag{2.29}$$

Then the insertion of this expansion in the Sverdrup relation and the potential vorticity equation yields a sequence of problems, whose details will be passed over quickly since they are very straightforward. The lowest order problem is, naturally, the purely wind-driven flow for which h is constant on lines of constant lower layer potential vorticity, and using the results from LPS

$$h^{(0)} = G(f/h_3^{(0)}) = f_2/q_3^{(0)} \tag{2.30}$$

while the O(b) problem in the lower layer, after some algebra becomes

$$\frac{\partial q_3^{(0)}}{\partial y}\left[\frac{\partial h^{(1)}}{\partial x} + \frac{f_2}{q_3^{(0)2}}\frac{\partial q_3^{(1)}}{\partial x}\right] - \frac{\partial q_3^{(0)}}{\partial x}\left[\frac{\partial h^{(1)}}{\partial y} + \frac{f_2}{q_3^{(0)2}}\frac{\partial q_3^{(1)}}{\partial y}\right] = q_3^{(0)2}\frac{U_2}{\gamma_3}. \tag{2.31}$$

Now

$$q_3^{(1)} = -\frac{f h_3^{(1)}}{h_3^{(0)2}} = -h_3^{(1)} q_3^{(0)2}/f$$

so that after the O(b) terms from (2.12) are equated, we finally obtain as an equation for $h^{(1)}$

$$\frac{\partial q_3^{(0)}}{\partial y}\frac{\partial}{\partial x}(P(\zeta)h^{(1)}) - \frac{\partial q_3^{(0)}}{\partial x}\frac{\partial}{\partial y}[P(\zeta)h^{(1)}] = -q_3^{(0)2}\frac{U_2}{\gamma_3} \tag{2.32}$$

where

$$P(\zeta) = \frac{1 + \Gamma_2(1-\zeta)^2}{\zeta(1-\zeta)\Gamma_2} \tag{2.33}$$

and $\zeta \equiv f/f_2$.

Equation (2.32) may be integrated using the method of characteristics. The characteristics of (2.32) are the isolines of $q_3^{(0)}$, the potential vorticity of the wind-driven flow in the absence of heating. Thus we find that

$$\frac{h^{(1)}}{h^{(0)}} = \frac{1}{P(\zeta)}\int_\zeta^1 \frac{U_2}{W_E}\frac{d\mu}{\mu^2}[1 + \Gamma_2(1-\mu)^2] \tag{2.34}$$

where the integral in (2.34) is understood to be carried out along the characteristic $q_3^{(0)}$ = constant. That is, if U_2/W_E is a function of x as well as y, then in (2.34) x must be written in terms of y (or f), i.e., in terms of the dummy variable μ. Thus, if U_2/W_E is a strong function of longitude, it is possible for the meridional velocity, in principle, to reverse in the ventilated zone. On the other hand, if U_2/W_E is a function only of f, then the integral is independent of the contour and depends only on the end point, i.e., $h^{(1)}/h^{(0)}$ is a function of f/f_2 alone. Indeed, this fact is what originally suggested the trial solution (2.13a, b). It is easy to verify that if the solution to (2.16) is expanded in a series for small b_2, the resulting series for θ,

$$\theta = \theta_0 + \theta_1 = (1-\zeta) - \zeta\int_\zeta^1 \frac{b_2(\mu)}{\mu^2}[1 + \Gamma_2(1-\mu)^2] \tag{2.35}$$

will yield, with (2.13) and (2.14) an expression identical to (2.34). This satisfactorily displays the validity of the guessed-at form, (2.13) as the general solution.

It must be realized that the solution (2.34), or (2.14), is valid only on ventilated streamlines for which the relations (2.13a, b) hold. This turns out to have important implications for the discussion of the circulation of the shadow zone.

3. The shadow zone

If H_3 is zero, i.e., if the depth of the deepest moving layer vanishes on the eastern boundary, the solution (2.13), (2.14) or (2.24), (2.25) will hold right up to the eastern wall. However, as discussed in LPS, if $H_3 \neq 0$, the streamline which north of $f = f_2$ flows due south along $x = x_E$ must separate from the eastern wall at $f = f_2$ and thread its way southeastward through the gyre

along, naturally, the line $h = H_3$. Again, for simplicity, I will restrict my discussion to the two-moving-layer model, i.e., I will let $f_1 \to 0$. Then the equation for the shadow zone boundary $\tilde{x}(f)$ can be obtained directly from (2.20), with the replacement of ξ with X_E [for which $D_0^2(\xi, f_2)$ vanishes] so that

$$\boxed{D_0^2[\tilde{x}(f), f] = H_3^2\Gamma_2\theta^2} \quad . \tag{3.1}$$

For $b_2 < 0$, i.e., for heating, θ is always greater than its adiabatic value when $b_2 = 0$. Since D_0^2 is an increasing function of $(X_E - x)$, this means that, in the case of heating, the shadow zone boundary is shifted westward. For example, for small b_2, it is easy to show, using (2.34) or (2.35), that

$$\frac{D_0^2}{H_3^2}[\tilde{x}(f), f] = \Gamma_2(1-\zeta)^2 - 2\Gamma_2\zeta(1-\zeta) \times \int_\zeta^1 \frac{b_2(\mu)}{\mu^2}[1 + \Gamma_2(1-\mu)^2]d\mu \tag{3.2}$$

where $\zeta = f/f_2$, so that the shift of the shadow zone is westward and $O(b_2)$ for $b_2(f) < 0$ (heating). The situation is shown in Fig. 6 where the shaded region is the new sliver of shadow zone exposed by the heating process.

I have not been able to find a complete solution valid in the shadow zone for arbitrarily large b_2 but progress can be made in the case of small b_2 which points to some general properties of the flow in that region; inferences which in some cases can be rigorously demonstrated. For small b_2, the solution to the set (2.11) and (2.12) may, as in section 2 be generated as a series

$$h = h^{(0)} + h^{(1)} + \cdots \tag{3.3}$$

in which superscripts refer to orders of smallness in b_2. In the case of the shadow zone, the O(1) solution is (LPS)

$$h_2^{(0)} = D_0\Gamma_2^{-1/2}$$
$$h^{(0)} = H_3 \tag{3.4a,b}$$

so that

$$q_3^{(0)} = f/(H_3 - h_2^{(0)}) = f/h_3^{(0)}. \tag{3.5}$$

Thus in the absence of buoyancy forcing, the fluid in the shadow zone is at rest in layer 3. Thus the O(b) problem for $h^{(1)}$ is of special importance because, although small, the resulting gradients in $h^{(1)}$ represent the entire, if relatively weak, circulation in the lower layer of the shadow zone. The substitution of (3.3) into (2.11), with the recognition that $h^{(0)}$ is constant quickly yields the problem for $h^{(1)}$ as

$$\frac{\partial h^{(1)}}{\partial x}\frac{\partial q_3^{(0)}}{\partial y} - \frac{\partial h^{(1)}}{\partial y}\frac{\partial q_3^{(0)}}{\partial x} = q_3^{(0)2}\frac{U_2}{\gamma_3} \tag{3.6}$$

from which $h^{(1)}$ may be calculated most conveniently by the method of characteristics.

The characteristics curves of (3.6) are simply the isolines of $q_3^{(0)}$, i.e., of the potential vorticity of the purely wind-driven circulation in the shadow zone. These isolines are shown in Fig. 6 as dotted lines in the shadow zone. Each isoline for a particular $q_3^{(0)}$ intersects the eastern boundary at $f = f_*$

$$f_* \equiv q_3^{(0)}H_3 = fH_3/h_3^{(0)}. \tag{3.7}$$

The small b_2 solution will therefore be determined on all such characteristic curves. Note, however, that these curves do not penetrate the shaded region in Fig. 6, which is the sliver, of width $O(b_2)$ which is opened up by the slight displacement westward of the shadow zone. The shaded region is penetrated by the $q_3^{(0)}$ lines emanating from the outcrop line but the solution (2.34) is valid only for fluid elements originating at the outcrop line and hence cannot be extended into the shadow zone (since $h = H_3$ represents the eastward limit of such fluid trajectories). Thus neither small buoyancy flux solution generated by the regular expansion in small U_2/w_E is valid in the shaded sliver of Fig. 6, which is an interesting feature of the circulation problem I will return to later.

Returning to (3.6), we may solve it by transforming (3.6) to the characteristic set by introducing the parameter τ such that

$$\frac{dx}{d\tau} = \frac{\partial q_3^{(0)}}{\partial y}$$
$$\frac{dy}{d\tau} = -\frac{\partial q_3^{(0)}}{\partial x}$$
$$\frac{dh^{(1)}}{d\tau} = q_3^{(0)2}\frac{U_2}{\gamma_3} \tag{3.8a,b,c}$$

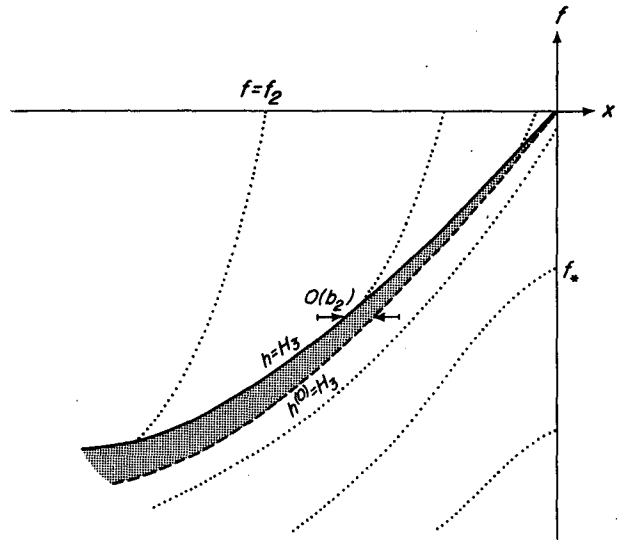

FIG. 6. The boundary between the eastern shadow zone and the ventilated region is determined by the streamline $h = H_3$. The dashed line shows the shadow zone boundary in the absence of heating. The dotted lines show the isolines of $q_3^{(0)}$, i.e., the potential vorticity contours of the purely wind-driven flow. On $x = x_E$ these contours intersect the eastern wall at $f = f_*(q_3^{(0)})$.

or

$$h^{(1)} = \int_0^\tau q_3^{(0)2} \frac{U_2}{\gamma_3} d\tau \tag{3.9}$$

where the integration in τ proceeds westward, from $\tau = 0$ which is the easternmost point where the isoline of $q_3^{(0)}$ intersects $x = X_E$ at $f = f_*$. With (3.8b), (3.8c) may be rewritten

$$h^{(1)} = \int_{y_*}^{y} q_3^{(0)2} \frac{U_2}{\gamma_3} \frac{dy}{dy/d\tau} = \int_y^{y_*} q_3^{(0)2} \frac{U_2}{\gamma_3} \frac{dy}{\partial q_3^{(0)}/\partial x} \tag{3.10}$$

where $f(y_*) = f_*$. Since

$$\frac{\partial q_3^{(0)}}{\partial x} = \frac{1}{f} q_3^{(0)2} \frac{\partial h_2^{(0)}}{\partial x}$$

$$h_1^{(0)} \frac{\partial h_1^{(0)}}{\partial x} = \frac{f^2}{\gamma_2 \beta} w_E,$$

it follows that

$$h^{(1)} = \int_f^{f_*} b_2 \Gamma_2 h_2^{(0)} \frac{df'}{f'} \tag{3.11}$$

where the integration in (3.11) is along the curve $x = x(f)$ along which $q_3^{(0)}$ is constant. Since

$$h_2^{(0)} = H_3 - f/q_3^{(0)},$$

(3.11) may be written in the form

$$\frac{h^{(1)}}{H_3} = \int_f^{f_*} b_2 \Gamma_2 \left[\frac{1}{f'} - \frac{1}{f_*}\right] df' \tag{3.12}$$

where, note, f_* is a *constant* along the contour of integration.

Consider the case where b_2 is a function of latitude, i.e., where the ratio U_2/w_E is independent of x. Then (3.12) is a function only of the end points f and f_*. Note that $f \leqslant f_*$. It follows directly that

$$\frac{\partial h^{(1)}}{\partial x} = \frac{f}{\gamma_3 \beta H_3} \frac{w_E}{(1 - f/f_*)} \int_f^{f_*} b_2(f') df'. \tag{3.13}$$

Thus if $b_2 < 0$ (heating), then in the subtropical gyre, where $w_E < 0$, $\partial h^{(1)}/\partial x$ must always be *positive*. That is, in the *old* shadow zone, i.e., excluding the shaded sliver in Fig. 6, the meridional flow in the once stagnant lower layer is *northward*.

This is the "direct cell" found numerically by Luyten and Stommel (1986b).

Similarly,

$$-\frac{\partial h^{(1)}}{\partial f} = H_3 b_2 \Gamma_2 \left[\frac{1}{f} - \frac{1}{f_*}\right] - \frac{\Gamma_2}{q_3^{(0)2}} \frac{\partial q_3^{(0)}}{\partial f} \int_f^{f_*} b_2 df'$$

$$= \frac{f_* - f}{q_3 f} \left[b_2 - \frac{f}{q_3^{(0)}} \frac{\partial q_3^{(0)}}{\partial f} \bar{b}_2\right], \tag{3.14}$$

where $\bar{b}_2 = (f_* - f)^{-1} \int_f^{f_*} b_2 df'$.

The sign of $-\partial h^{(1)}/\partial f$ is not immediately obvious. The first term on the right-hand side is negative if $b_2 < 0$ and depends on the *local* value of b_2. The second term will be positive in the heating case as long as $\partial q_3^{(0)}/\partial y > 0$, i.e., as long as the forcing has not reversed the "normal" sense of the potential vorticity gradient. This term depends on the integral quantity $\bar{b}_2$. Thus, if $b_2 \to 0$ as $f \to 0$, the second term will tend to dominate for small f while the sign of the sum may be reversed at more northern latitudes if

$$-b_2 > \frac{f}{q_3^{(0)}} \frac{\partial q_3^{(0)}}{\partial f} (-\bar{b}_2).$$

In any case, it can be shown that $h^{(1)}$ increases along the old shadow zone boundary so flow crosses northwestward into the sliver. Thus in the region excluding the sliver, the buoyancy-driven circulation consists of a broad northeasterly flow turning to meet the sliver-shadow zone boundary.

It was noted in section 2 that, if b_2 were a *constant*, then relatively simple analytical solutions could be found in the ventilated zone. A similar and perhaps more illuminating simplification occurs in the shadow zone. Actually, this is a pretty fair idealization in the shadow zone since, in the shadow zone where the upper layer to O(1) carries the total Sverdrup transport, the gradients of $h_3^{(0)}$, $h_2^{(0)}$, etc., are relatively great. Thus b_2 in comparison will appear as a fairly slowly varying function in (3.12) and temporarily I wish to consider the idealization of constant b_2. In that case (3.12) implies that

$$h^{(1)} = b_2 \Gamma_2 H_3 \left[\ln \frac{f_*}{f} - (1 - f/f_*)\right]; \tag{3.15}$$

hence $h^{(1)}$ is a function only of f/f_*. But from (3.7), this implies that $h^{(1)}$ is a function only of $h_3^{(0)}$, or of $h_2^{(0)}$. That is, to lowest order, when b_2 is constant, the contours of layer thickness in the two layers coincide. Returning to (3.6), this implies that the twisting terms $\nabla h^{(1)} \times \nabla h_3^{(0)}$ are identically zero so that (3.6) reduces to

$$\boxed{\beta v_3^{(1)} h_3^{(0)} = f U_2}. \tag{3.16}$$

Thus the northward meridional transport in the formerly stagnant zone may be computed directly in terms of the buoyancy flux without regard to the wind forcing. *The buoyancy mode becomes decoupled from the wind-driven circulation.* The form (3.16) is so simple and striking that it is natural to ask whether the result can be generalized to arbitrarily large, but constant, values of b_2. The answer is yes.

For the twisting in (2.11) to vanish in general, we must have (noting that $h_3 = h - h_3$)

$$h = \mathscr{H}(h_2) \tag{3.17}$$

where $\mathscr{H}$ is an arbitrary function. If (3.17) is to hold, (2.11) and (2.12) require

$$h \frac{\partial h}{\partial x} + \Gamma_2 h_2 \frac{\partial h_2}{\partial x} = \frac{1}{2} \frac{\partial D_0^2}{\partial x} \tag{3.18}$$

$$\beta \frac{\partial h}{\partial x}(h - h_2) = \frac{f^2}{\gamma_3} U_2. \tag{3.19}$$

If we note that $\partial h/\partial x = \mathscr{H}' \partial h_2/\partial x$ where $\mathscr{H}'$ is the derivative of $\mathscr{H}$ with respect to its argument, (3.18) and (3.19) require as a condition on $\mathscr{H}$ that

$$\boxed{\mathscr{H}'[\mathscr{H}(1 - b_2) - h_2] - b_2\Gamma_2 h_2 = 0} \tag{3.20}$$

such that, at $x = X_E$ where $h_2 = 0$, $h = H_3$, or

$$\mathscr{H}(0) = H_3. \tag{3.21}$$

As long as b_2 is constant, solutions to (3.20) and (3.21) can be found, usually numerically. For $b_2 = 0$, the solution is $\mathscr{H} = H_3$, i.e., a motionless shadow zone as in LPS. For small b_2, the expansion of (3.20) yields

$$\mathscr{H}(h_2) = H_3 - b_2\Gamma_2[h_2 + H_3 \ln(1 - h_2/H_3)] + O(b_2)^2 \tag{3.22}$$

in perfect agreement with (3.15). The exact form of $\mathscr{H}(h_2)$ is not nearly as important as the existence of the functional relationship, for it implies that (3.16) may be rewritten

$$\boxed{\beta v_3 h_3 = f U_2} \tag{3.16'}$$

for all constant b_2. Thus, if b_2 can be idealized as a constant, the eastern portion of the shadow zone will lack a beta-spiral, i.e., the flow paths will be antiparallel in the two layers, and the meridional transport in the lower layer given by (3.16') takes the form of a single layer Sverdrup relation (2.6) with the buoyancy flux replacing the Ekman pumping, allowing an independent determination of the meridional transports in the two layers.

Let us return to the case of small, variable b_2 for which the solution for $h^{(1)}$ is given by (3.12). As noted above, the solution is not valid in the shaded sliver of Fig. 6. This is as it must be, for as previously remarked, the buoyancy-driven flow in the *old* shadow zone is everywhere northeastward and there must be a return branch for mass balance. The flow in the ventilated zone is southward but consists of water whose origin is distinct from shadow zone water. The only remaining possibility is that the return branch be channeled through the sliver opened up by the buoyancy flux. The situation is shown in Fig. 7. The flow in the old shadow zone has velocities in layer 3 of $O(b_2)$ and thus a total northward transport of $O(b_2)$. The depth of the bottom of layer 3 is shown in a zonal section in Fig. 7a; $h^{(1)}$ is negative and decreases from zero at $x = X_E$. The depth slowly decreases from H_3 on X_E to a value on $O(b_2)$ less on the eastern edge of the sliver. *Along* the eastern edge of the sliver, $h^{(1)}$ increases northward as shown in Fig. 7b. Nevertheless, the western boundary of the sliver is the new $h = H_3$ contour. Hence from the point P to the point A, h_3 must increase to reattain the value H_3 on A. Since this occurs over a width of only $O(b_2)$, it implies velocities in the sliver which are $O(1)$ and flowing nearly parallel to the edge of the ventilated zone as indicated in Fig. 7. Since the velocities are $O(1)$ to balance the mass flux, this implies that for small b_2, the buoyancy is unable at lowest order to affect the potential vorticity of the flow in the sliver. That is, since $\partial h/\partial x$ and $\partial h/\partial y$ are $O(1)$ in this region [although Δh is only $O(b_2)$], it follows from (2.11) that for small U_2, to lowest order

$$f/h_3 = G(h) \tag{3.23}$$

while if G is known, the solution is completed with the aid of (2.12). To lowest order, then, the dynamics in the sliver is the same as the $O(1)$ dynamics of the ventilated region. There is, however, a significant difference. Whereas in the ventilated zone, the function G is determined at the outcrop latitude, in the buoyancy sliver the relation between potential vorticity and depth is determined along the eastern boundary of the sliver, i.e., along the old shadow zone boundary. Note that the outermost $h^{(1)}$ contour $h^{(1)} = 0$, corresponding to the outer rim of the buoyancy circulation, hugs the eastern boundary and intersects the sliver at $f = f_2$. As it turns southward it has $q_3 = f/H_3$, while conservation of q_3 and the Sverdrup relation, identical constraints as the $O(1)$ ventilated dynamics, ensure that the outer streamline of the return flow in the sliver is coincident with the new shadow zone boundary $h = H_3$. Thus we are guaranteed that the return flow is entirely contained in the buoyancy sliver.

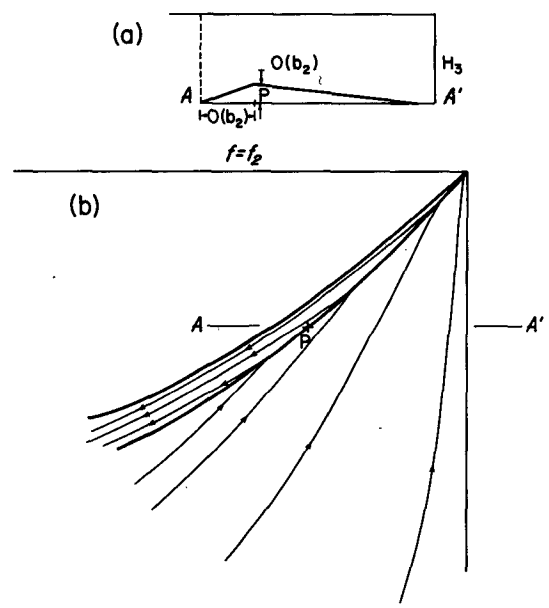

FIG. 7. A schematic of the circulation in the lower layer of the shadow zone. The buoyancy-driven flow with velocities of $O(b_2)$ sweeps northeastward over a broad $O(1)$ zone. The water is returned in a sliver of width $O(b_2)$ implying $O(1)$ velocities on the eastern edge of the ventilated zone. The upper panel shows a schematic of the depth of the lowest moving layer.

Since $h^{(1)}$ is known along the eastern boundary of the sliver [we merely set $f_* = f_2$ in (3.12)], the matching implied by (3.23) may in principle be carried out in the same manner as in Pedlosky (1983) where efflux from an eastern boundary layer was matched to the ventilated interior. However, because of the curved boundary in the present case, the actual matching becomes prohibitively complex and, since the qualitative nature of the flow is already clear as shown in Fig. 7, it seems hardly pertinent to the discussion to proceed further.

There is a final and important link between the shadow zone and the ventilated region. We noted in section 2 that pinch-off would occur within the ventilated region on the latitude circle, $f = f_c$, for which $\theta(f_c) = 1$. Were the ocean to extend an infinite distance westward from X_E, pinch-off would always occur. However, for $L = X_E - X_w$ and bounded, it is possible that the latitude of pinch-off always lies south of the shadow zone boundary for $X_w < x \leqslant X_E$, and so no pinch-off would occur in the basin. For pinch-off to occur then, it is required that

$$\tilde{x}(f_c) > X_w \tag{3.24}$$

where $\tilde{x}(f)$ is the coordinate of the shadow zone boundary. Since D_0^2 is a monotonically increasing function of $X_E - x$, where $w_E < 0$, it follows that (3.24) implies

$$D_0^2(X_w, f_c) > D_0^2[\tilde{x}(f_c), f_c] = H_3^2\Gamma_2. \tag{3.25}$$

If w_E were a function of f only, the condition for pinch-off thus requires

$$L = X_E - X_w > \frac{H_3^2\Gamma_2\beta(f_c)\gamma_3}{2f_c^2[-w_E(f_c)]}.$$

Pinch-off is therefore favored by small H_3, which is intuitively obvious, and large Ekman pumping, which while not obvious is required in order that $\tilde{x}(f)$ penetrate sufficiently southward.

4. Discussion

The action of buoyancy flux produces rather important alterations of the thermocline circulation than that found for the purely wind-driven case analyzed in LPS. Yet, within the ventilated zone, it is remarkable how similar the overall structure of the thermocline fields are in the two cases. In the two-layer model, for example, a single function, $\theta(f)$, which is determined by the ODE (2.16) is sufficient to describe the structural effects of buoyancy flux in the ventilated region. The westward shift of the streamlines for the heated subtropical gyre, cold layer pinch-off, and an enhanced shadow zone are all connected to this simple latitude structure function.

Although the analytical solution is incomplete in the shadow zone, the case of small buoyancy flux has revealed a flow configuration with a rich structure containing a deep cyclonic gyre with asymmetric branches. The appearance of a largely potential vorticity conserving flow on the border of the ventilated zone, which is needed to return the broader northward "direct" cell in the shadow zone, is a striking feature of the analysis. Many of the qualitative features exposed by the analysis are already present in the very interesting numerical calculations of Luyten and Stommel (1986b) but, of course, it is especially useful to have analytical representations of the dynamical fields.

An important qualification must be realized. In principle, the right-hand side of (2.7) can represent *any* baroclinic source of potential vorticity which leaves (2.6), the Sverdrup relation, unaltered. In that sense the results of the calculations presented here could be thought to apply to any such forcing and not just a large-scale buoyancy flux, e.g., the rectified heat flux of baroclinically unstable waves could, in principle, similarly enter. However, just this appeal to generality exposes the weakness of the buoyancy model described here. Whereas the Ekman flux is fairly clearly related to the externally imposed wind stress, in actuality, the buoyancy fluxes, U_n, should be connected not only to external heating, but to the structure of (at least) the oceanic density field. Rather than being imposed as external fields, the U_n should more likely be part of the solution to be calculated. Therefore, the present analysis must be considered as only a first step in an investigation of the buoyancy-driven circulation and clearly lacks the dynamical "cleanliness" of the Ekman-driven flow.

Acknowledgments. It is a pleasure to acknowledge the many helpful discussions about the buoyancy-driven circulation problem with Henry Stommel who kindly also showed me preprints of his and Jim Luyten's work. I wish to also acknowledge an anonymous reviewer whose careful reading of the original manuscript helped correct numerous small errors in the text. This research was supported in part by the National Science Foundation's Division of Atmospheric Sciences.

REFERENCES

Luyten, J. R., and H. Stommel, 1986a: A beta control of buoyancy-driven geostrophic flows. *Tellus*, **38A**, 88–91.

——, and ——, 1986b: Gyres driven by combined wind and buoyancy flux. *J. Phys. Oceanogr.*, **16** (in press).

——, J. Pedlosky and H. Stommel, 1983: The ventilated thermocline. *J. Phys. Oceanogr.*, **13**, 292–309.

Pedlosky, J., 1983: Eastern boundary ventilation and the structure of the thermocline. *J. Phys. Oceanogr.*, **13**, 2038–2044.

——, W. Smith and J. R. Luyten, 1984: On the dynamics of the coupled mixed layer-thermocline system and the determination of the oceanic surface density. *J. Phys. Oceanogr.*, **14**, 1159–1171.

Rhines, P. B., and W. R. Young, 1981: A theory of the wind-driven circulation. I. Mid-ocean gyres. *J. Mar. Res.*, **40**(Suppl.), 559–596.